

# 16.901 Project #2

## Sample Solution

### 1 Background

We will simulate the compressible inviscid flow through a varying-area duct in this project. The goal is to gain some understanding of the convergence behavior of Computational Fluid Dynamics algorithms applied to this problem for varying mesh size and under different flow conditions. In particular, we will use a first-order upwind spatial approximation with a Forward Euler timestep algorithm.

The cross-sectional area of the duct has a constant area section, a smooth converging section to a throat, a smooth diverging section to a final constant area section. The specific geometry is given by,

$$\begin{aligned} \text{For } 0 \leq x \leq x_1 : \quad A(x) &= A_0, \\ \text{For } x_1 \leq x \leq x_2 : \quad A(x) &= A_0 + \frac{1}{2}(A_1 - A_0) \{1 - \cos[\pi(x - x_1)/(x_2 - x_1)]\}, \\ \text{For } x_2 \leq x \leq x_3 : \quad A(x) &= A_1 + \frac{1}{2}(A_2 - A_1) \{1 - \cos[\pi(x - x_2)/(x_3 - x_2)]\}, \\ \text{For } x_3 \leq x \leq x_4 : \quad A(x) &= A_2. \end{aligned}$$

For the problem in this project, we will set:

$$\begin{aligned} x_1 &= 1 \text{ m} \\ x_2 &= 2 \text{ m} \\ x_3 &= 3 \text{ m} \\ x_4 &= 4 \text{ m} \\ A_0 &= 10 \text{ m}^2 \\ A_1 &= 8 \text{ m}^2 \\ A_2 &= 12 \text{ m}^2 \end{aligned}$$

The flow through the duct will be set by a pressure difference occurring from inlet to the outlet. Specifically, at the inlet, we will assume that the total pressure and the total temperature are equal to sea level atmospheric conditions:

$$\begin{aligned} P_{0inlet} &= 101,327 \text{ N/m}^2 \\ T_{0inlet} &= 288.15 \text{ K} \end{aligned}$$

At the outlet, we will solve the flow for three different static pressures specifically,

$$P_{outlet}/P_{0inlet} = 0.70, 0.90, \text{ and } 0.995.$$

The quasi-1D Euler equations can be written in a control volume form as,

$$\frac{d}{dt} \int_{x_L}^{x_R} UA \, dx + F(U(x_L))A(x_L) - F(U(x_R))A(x_R) = S \quad (1)$$

where  $U$  and  $F$  are,

$$U = \begin{pmatrix} \rho \\ \rho u \\ \rho E \end{pmatrix}, \quad F = \begin{pmatrix} \rho u \\ \rho u^2 + p \\ \rho u H \end{pmatrix},$$

and  $S$  is a source term vector due to the area-variation,

$$S = \begin{pmatrix} 0 \\ \int_{x_L}^{x_R} p dA \\ 0 \end{pmatrix}.$$

As described in Homework #4,  $\rho$  is the density,  $u$  is the flow velocity,  $p$  is the pressure, and  $E$  is the total energy.  $H$  is the total enthalpy and is related to the previous quantities by,

$$H = E + \frac{p}{\rho}.$$

Note, the total energy ( $E$ ) and total enthalpy ( $H$ ) are related to the energy ( $e$ ) and enthalpy ( $h$ ) by the following,

$$\begin{aligned} E &= e + \frac{1}{2}u^2 \\ H &= h + \frac{1}{2}u^2 \end{aligned}$$

To close this set of equations, we will assume the working fluid is air and can be assumed to be an ideal, perfect gas. In this case, the state equations for the pressure and energy are,

$$p = \rho RT, \tag{2}$$

$$e = c_v T, \tag{3}$$

where  $R$  is the gas constant,  $T$  is the temperature, and  $c_v$  is the specific heat at constant volume. Another useful thermodynamic quantity is the specific heat at constant pressure,  $c_p$ , which is related to  $R$  and  $c_v$  by,

$$c_p - c_v = R.$$

Also, the ratio of specific heats  $\gamma = c_p/c_v$ . For air, we will assume that,

$$\gamma = 1.4 \quad R = 287.06 \text{ m}^2(\text{s}^2\text{K})^{-1}$$

As shown in Homework #4, the pressure can be related to the conservative state vector by,

$$p = (\gamma - 1) \left( \rho E - \frac{1}{2}\rho u^2 \right).$$

Finally, for a perfect gas, the speed of sound,  $c$  is given by,

$$c = \sqrt{\frac{\gamma p}{\rho}}.$$

## 1.1 Discrete Equations for Interior Cells

We begin by dividing the duct into  $N_x$  equal divisions (producing  $N_x$  cells). The unknowns will be the average-values of the state vector  $U$  in each cell, i.e. you will be solving for  $U_j$  for  $j = 1$  to  $N_x$ .

For every cell in the interior of the domain (i.e.  $j = 2$  to  $N_x - 1$ ), we will use a discrete form of Equation (1) to find a new value at every iteration. Specifically, the discretization which you need to implement for the project is,

$$\frac{U_j^{n+1} - U_j^n}{\Delta t^n} V_j + R_j^n = 0, \tag{4}$$

where  $R_j^n$  is the local residual vector for cell  $j$  at iteration  $n$ . This local residual is defined as,

$$R_j^n = \hat{F}(U_j^n, U_{j+1}^n) A_{j+\frac{1}{2}} - \hat{F}(U_{j-1}^n, U_j^n) A_{j-\frac{1}{2}} - S_j^n. \tag{5}$$

The function  $\hat{F}$  has been written already (as a Matlab<sup>®</sup> script called **Fupwind.m**) and is available on the course website as an additional attachment. This function, known as a flux function, takes the left and right state vector (and the value of  $\gamma$ ) at a face between two cells, and returns the flux which has been determined by properly upwinding the states to the face. The resulting difference approximation would be equivalent to a standard 1st order upwind discretization if the problem were just scalar convection instead of the Euler equations. NOTE: the order in which the states are given in the flux function input list is important. Do not reverse them!

The source term is approximated as,

$$S_j^n = \begin{pmatrix} 0 \\ p_j^n (A_{j+\frac{1}{2}} - A_{j-\frac{1}{2}}) \\ 0 \end{pmatrix}. \quad (6)$$

Also,  $V_j$  is the volume of cell  $j$  and should be approximated by,

$$V_j = \frac{1}{2}(A_{j-\frac{1}{2}} + A_{j+\frac{1}{2}})\Delta x.$$

## 1.2 Timestep Calculation

The timestep will be set with the following CFL condition,

$$\Delta t^n = CFL \min_{j=1}^{N_x} (\Delta t_j^n),$$

where,

$$\Delta t_j^n = \frac{\Delta x}{|u_j| + c_j}.$$

While you can experiment with the CFL number you use to determine the timestep, von Neumann stability analysis suggests that the  $CFL \leq 1$  to remain stable. My suggestion would be to use a  $CFL = 0.9$  for all of the simulations you will perform in this project.

## 1.3 Boundary Condition Implementation

At the inlet, we need to determine the state vector  $U_1$  by imposing boundary conditions. Specifically, we need to have three pieces of information that can be manipulated to uniquely determine the state vector (since the state vector has three components). We assume the inlet flow to be subsonic, as a result, only two pieces of information may be set while the third piece of information must come from the interior states. The two pieces of information we will set are the total pressure and total temperature at the inlet. From cell  $j = 2$ , we will use the velocity,  $u_2$ . Thus, these three pieces of information can be used to determine the state vector  $U_1$ , i.e.

$$U_1 = U(P_{0inlet}, T_{0inlet}, u_2)$$

Note: by this notation, it is meant that given the total pressure, total temperature, and velocity, the entire state vector can be determined.

At the outlet, we also will assume a subsonic flow. In this situation, we specify only one condition and take two pieces of information from the interior. For this assignment, we will set the static pressure and take the entropy,  $S$ , and  $J_+$  (known as Riemann invariant) from the interior. A definition of entropy for an ideal gas is,

$$S = \frac{p}{\rho^\gamma}.$$

The definition of  $J_+$  is,

$$J_+ = u + 2\frac{c}{\gamma - 1}.$$

Thus, to find the outlet state vector, we need to combine this information,

$$U_{N_x} = U(p_{outlet}, S_{N_x-1}, J_{+N_x-1})$$

## 1.4 Initial Condition

For all of the cases run, use an initial of stagnation flow from the inlet conditions. That is, set  $u = 0$ ,  $p = P_{0inlet}$ , and  $T = T_{0inlet}$  everywhere in the duct prior to the first iteration.

# 2 Assignment

## 2.1 Implementation of Discretization

The source code for which solves the Quasi-1D Euler equations is available on the 16.901 web site with this solution.

## 2.2 Residual Convergence Check

The convergence check should satisfy two properties:

- As the discrete solution is approached, the residual measure should also approach zero.
- The residual measure should not be strongly dependent on the number of cells used to solve a given problem.

To develop our measure, we propose the following analytic quantity:

$$RMS(t) = \sqrt{\int_0^L \left(\frac{d\rho}{dt}\right)^2 dx}.$$

Since this integral is only a function of time for a given problem, then a discrete version of this should behave in approximately the same manner and not be strongly dependent on the number of cells. The discrete version can be derived as follows,

$$\begin{aligned} RMS^n &= \sqrt{\sum_{i=2}^{N_x-1} \left(\frac{\rho_i^{n+1} - \rho_i^n}{\Delta t}\right)^2 \Delta x}, \\ &= \sqrt{\sum_{i=2}^{N_x-1} (R_{mass_j}^n / V_j)^2 \Delta x}. \end{aligned}$$

Note: the sum is only from  $i = 2$  to  $N_x - 1$  because the first and last cells do not have residuals as the boundary conditions are imposed at these locations.

To demonstrate the relatively small sensitivity to grid size, the results from the  $p_{outlet}/P_{0inlet} = 0.70$  cases for all grids can be seen in Figures 1-4. The RMS histories show clearly that the absolute levels are the same for all grid sizes, with finer grids having somewhat more detailed variations of the RMS residual and taking more iterations to converge (this longer convergence will be discussed below).

The criterion used to determine convergence was that the ratio of the current RMS residual to the maximum RMS residual for all iterations is less than  $10^{-4}$ :

$$\text{Convergence tolerance: } \frac{RMS^n}{\max_{k=1}^n RMS^k} \leq 10^{-4}.$$

This level was determined to be adequate by observing the behavior of two outputs of the simulation, specifically, the outlet total pressure  $P_{0outlet}$  and the outlet mass flow rate  $\dot{m}_{outlet}$ . As shown by the transonic results in Figures 1-4, these outputs have approached an asymptotic value by the iteration at which the convergence tolerance criteria was met. Thus, the RMS-based convergence check seems reasonable. Similar behaviors were observed in all simulations.

## 2.3 Simulations

The Mach number distributions for the three different pressure ratios using all grids are shown in Figures 5-7. Also, the behavior of the total pressure ratio  $P_{0outlet}/P_{0inlet}$  and the outlet massflow rate versus pressure ratio  $p_{outlet}/P_{0inlet}$  for all four grids are shown in Figures 8 and 9, respectively.

With respect to grid size, the solutions are clearly converging, however, the two flows with pressure ratios near one are still changing appreciably with grid size even in moving from  $N_x = 80$  to  $N_x = 160$ . For example, for  $p_{outlet}/P_{0inlet} = 0.9$ , the mass flow rate changes by approximately 2% in moving from  $N_x = 80$  to  $N_x = 160$ . However, for the  $p_{outlet}/P_{0inlet} = 0.7$ , the mass flow rate changes only 0.005%. The reason the flow rate is largely unaffected by numerical errors in this larger pressure drop case is that the flow is transonic and therefore is choked. Since the Mach number is well above the limiting choking condition which occurs when  $M = 1$ , numerical errors will have only a small impact on the flow rate. This behavior can be confirmed from the Mach number distributions in Figure 5 and 6. For the choked case, the Mach number distribution changes only near the shock. However, for the lower Mach number case, the entire Mach number distribution is shifting upward, therefore representing an increasing flow rate.

## 2.4 Iterations and Timings

For the 12 simulations run in the previous section, the number of iterations and the CPU time required to reach convergence are given in Tables 1 and 2. As can be observed, the number of iterations and CPU time increase with increasing grid size ( $N_x$ ) and as  $p_{outlet}/P_{0inlet} \rightarrow 1$ .

The dependence of the number of iterations on grid size can be explained as follows. The time step is limited by the CFL condition such that,

$$\Delta t \propto \frac{\Delta x}{\bar{u} + \bar{c}},$$

where  $\bar{u}$  and  $\bar{c}$  are typical (i.e. average) values of the flow velocity and speed of sound throughout the domain. Note, we assume that  $\bar{u} > 0$ . Thus, as the spacing is decreased, the timestep is also decreased. Since the simulation is time-marched to a 'steady' answer, there will be some finite time,  $T$ , at which the change in the state vector will be small, independent of the mesh resolution. As a result, the number of iterations for convergence will be,

$$N_{iters} = \frac{T}{\Delta t} \propto \frac{T(\bar{u} + \bar{c})}{\Delta x} = N_x \frac{T(\bar{u} + \bar{c})}{L}.$$

As a result, one would expect that the number of iterations would double if the number of cells doubled. This trend is clearly observed in Table 1.

The dependence of the CPU time on grid size can be explained as follows. As we saw, the number of iterations is expected to scale with the number of cells. Furthermore, the work required for a single iteration also scales with the number of cells as a residual is calculated for every cell. Thus, we expect,

$$\begin{aligned} Work &= \frac{Work}{Iter} \times N_{iters} \\ &\propto N_x \times N_x \frac{T(\bar{u} + \bar{c})}{L} = N_x^2 \frac{T(\bar{u} + \bar{c})}{L}. \end{aligned}$$

Thus, the work scales with  $N_x^2$ . Clearly, the CPU timings in Table 2 show this dependence.

The dependence of the number of iterations and the CPU time on  $p_{outlet}/P_{0inlet}$  can be explained as follows. The time for convergence,  $T$ , which we discussed above, will require that all errors have propagated through the domain. Thus, the slowest-moving wave will tend to set  $T$ . If we assume that the average flow is subsonic with  $0 < \bar{u} < \bar{c}$ , then,

$$T \propto \frac{L}{\min(\bar{c} - \bar{u}, \bar{u})}$$

Thus, the number of iterations for convergence should behave as,

$$N_{iters} \propto N_x \frac{\bar{u} + \bar{c}}{\min(\bar{c} - \bar{u}, \bar{u})}.$$

$N_x$	$p_{outlet}/P_{0inlet}$		
	0.70	0.90	0.995
20	368	791	1746
40	768	1760	3559
80	1584	3705	6592
160	3227	7117	14316

Table 1: Iteration requirements versus grid size ( $N_x$ ) and pressure ratio.

$N_x$	$p_{outlet}/P_{0inlet}$		
	0.70	0.90	0.995
20	2.3	5.1	11.2
40	9.4	22.3	43.7
80	38.1	89.7	159.6
160	153.1	336.6	683.7

Table 2: CPU time requirements versus grid size ( $N_x$ ) and pressure ratio.

Or, re-writing this in terms of the average-Mach number gives,

$$N_{iters} \propto N_x \frac{\bar{M} + 1}{\min(1 - \bar{M}, \bar{M})}.$$

From the plots in Figures 5-7, we (very crudely) approximate the average-Mach numbers as follows:

$$\begin{aligned} \bar{M}(p_{outlet}/P_{0inlet} = 0.7) &\approx 0.7 \\ \bar{M}(p_{outlet}/P_{0inlet} = 0.9) &\approx 0.5 \\ \bar{M}(p_{outlet}/P_{0inlet} = 0.995) &\approx 0.1 \end{aligned}$$

Thus, we expect the number is iterations to scale as follows:

$$\begin{aligned} N_{iters}(p_{outlet}/P_{0inlet} = 0.7) &\propto 5.7N_x \\ N_{iters}(p_{outlet}/P_{0inlet} = 0.9) &\propto 3N_x \\ N_{iters}(p_{outlet}/P_{0inlet} = 0.995) &\propto 11N_x \end{aligned}$$

These trends are not quite observed. Clearly, the number of iterations for the  $p_{outlet}/P_{0inlet} = 0.995$  case is the largest as predicted by the analysis. However, the transonic shocked case is the fastest converging, which is not predicted by the analysis. My guess is that the chocked nature of the transonic flow helps converge the flow; however, this has not been confirmed.

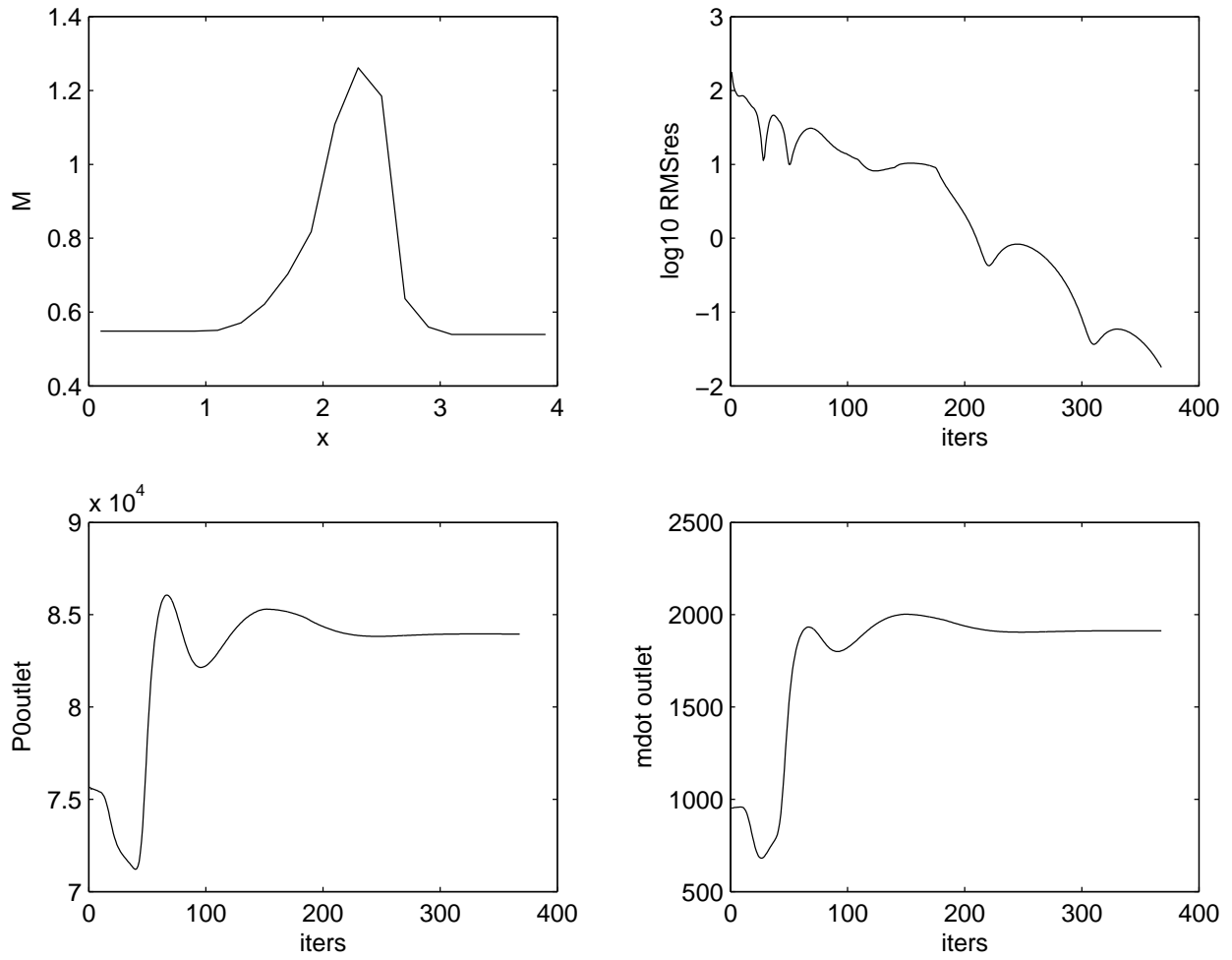


Figure 1: Mach number distribution and convergence behavior for  $p_{\text{outlet}}/P_{0\text{inlet}} = 0.7$  and  $N_x = 20$ .

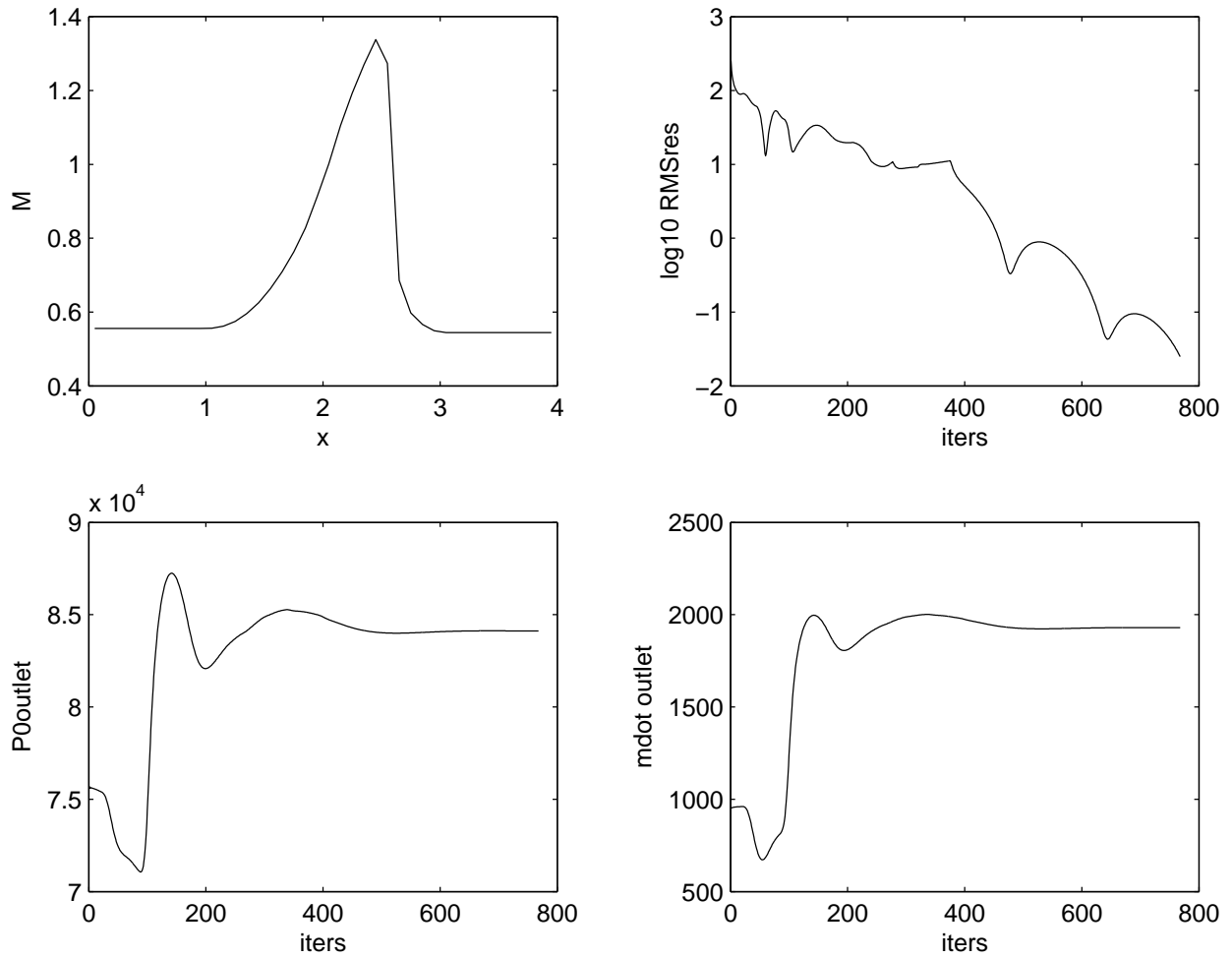


Figure 2: Mach number distribution and convergence behavior for  $p_{outlet}/P_{inlet} = 0.7$  and  $N_x = 40$ .



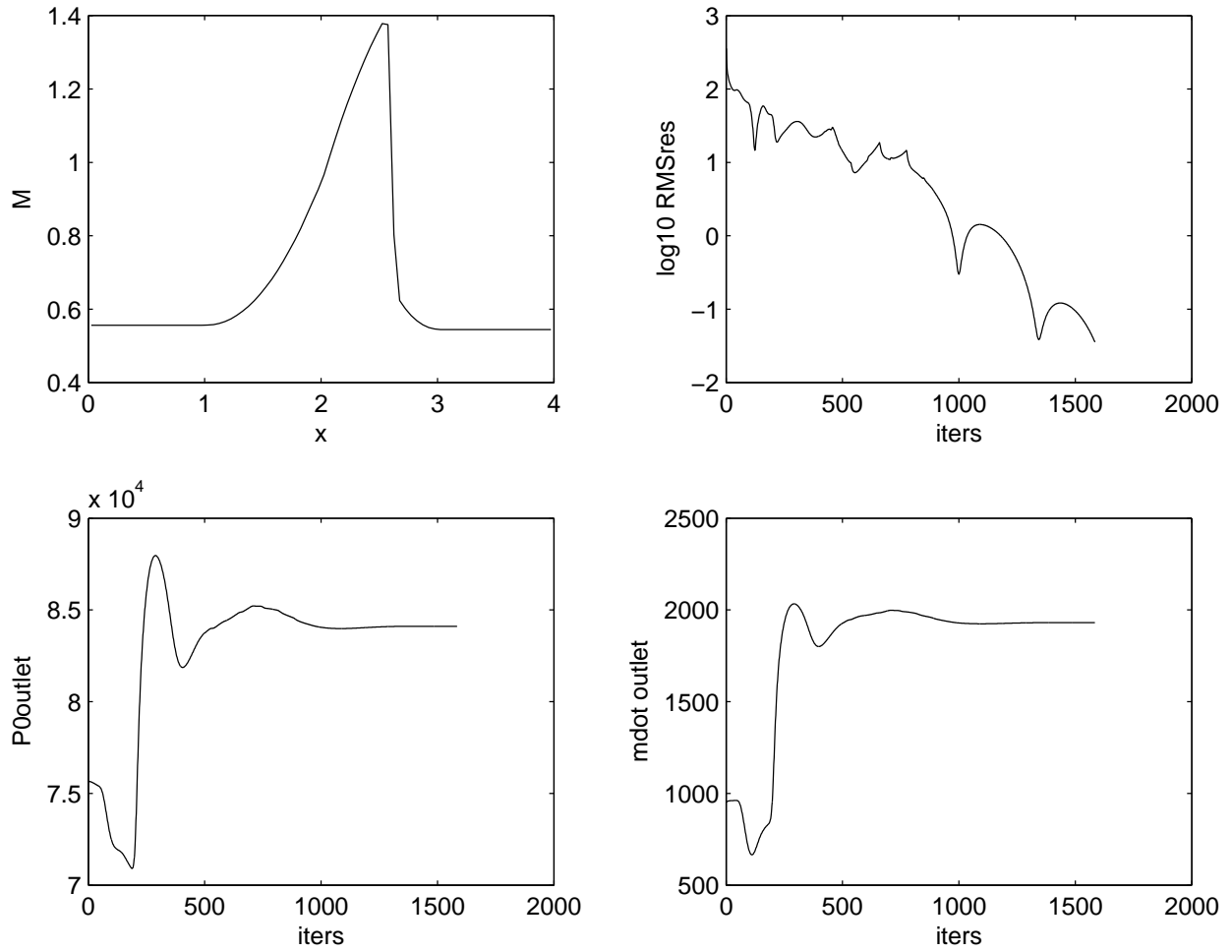


Figure 3: Mach number distribution and convergence behavior for  $p_{\text{outlet}}/P_{0\text{inlet}} = 0.7$  and  $N_x = 80$ .

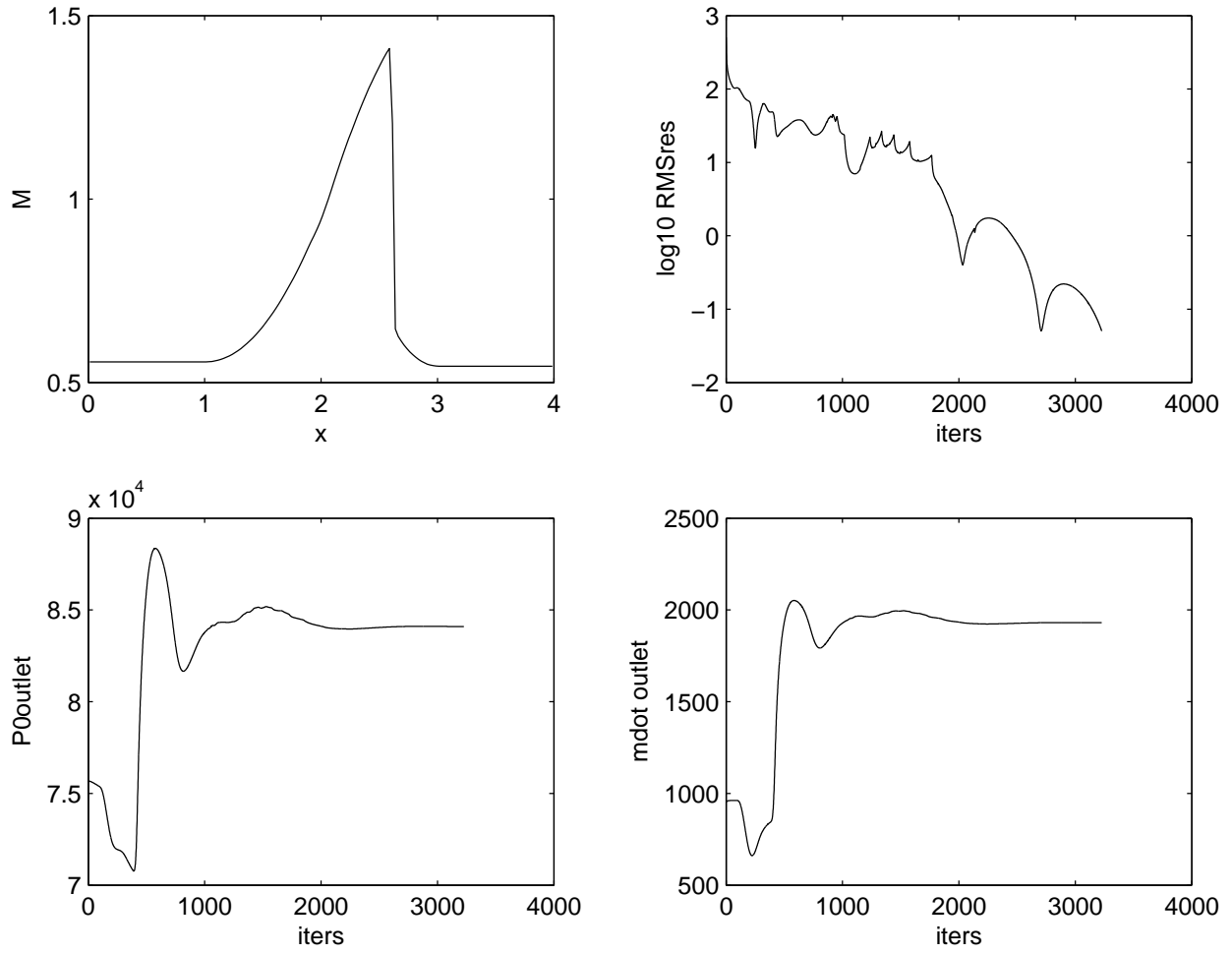


Figure 4: Mach number distribution and convergence behavior for  $p_{outlet}/P_{0inlet} = 0.7$  and  $N_x = 160$ .

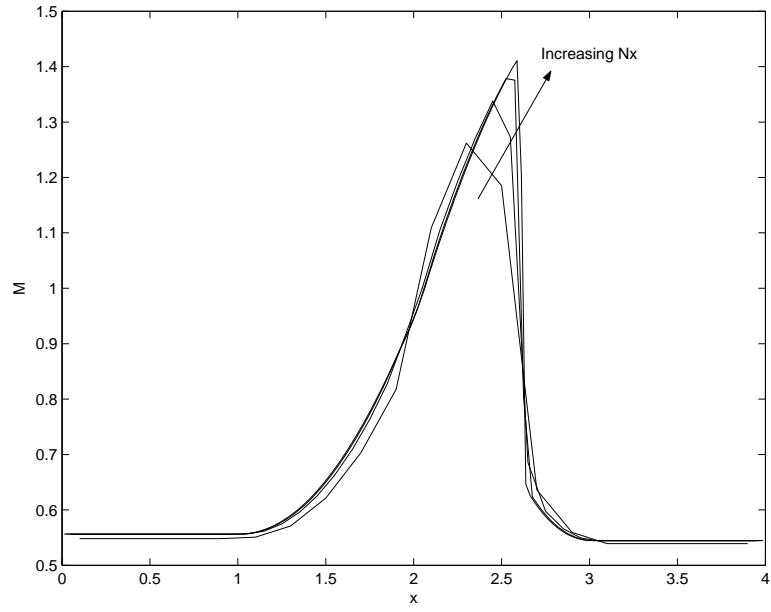


Figure 5: Mach number distribution for  $p_{outlet}/P_{0inlet} = 0.7$  for all grids.

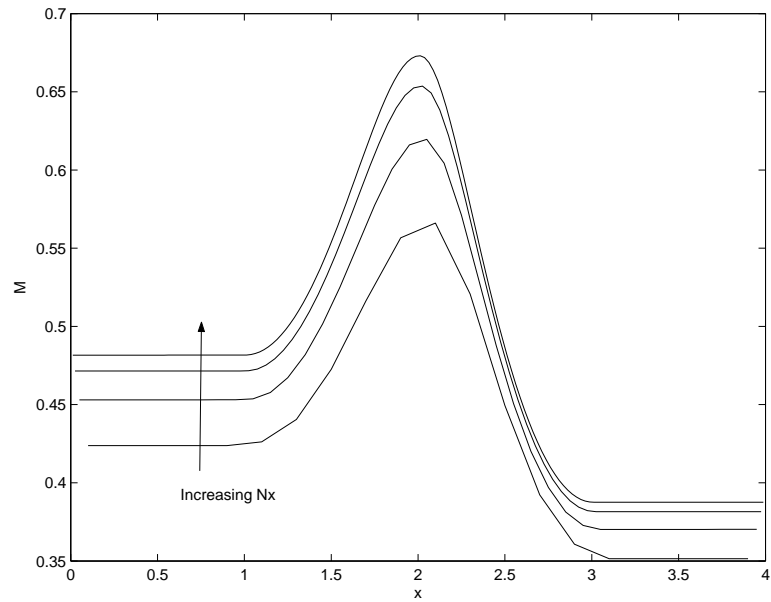


Figure 6: Mach number distribution for  $p_{outlet}/P_{0inlet} = 0.9$  for all grids.

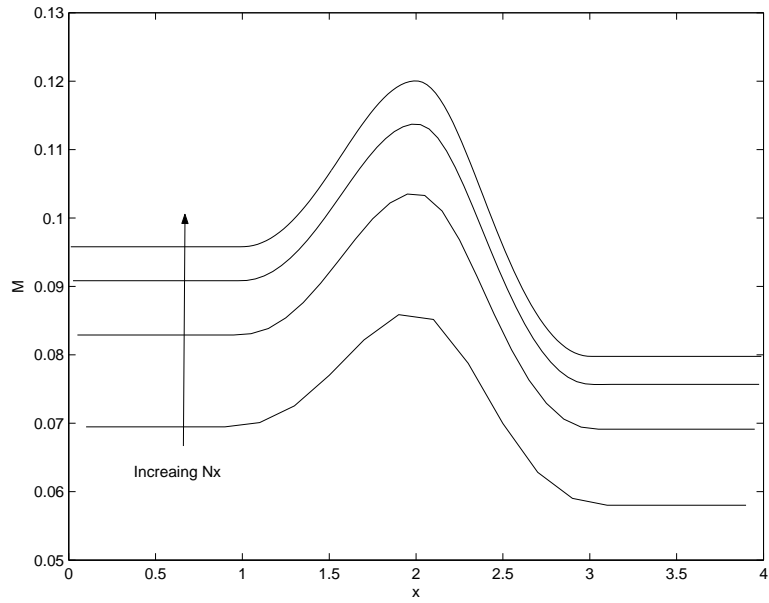


Figure 7: Mach number distribution for  $p_{outlet}/P_{0inlet} = 0.995$  for all grids.

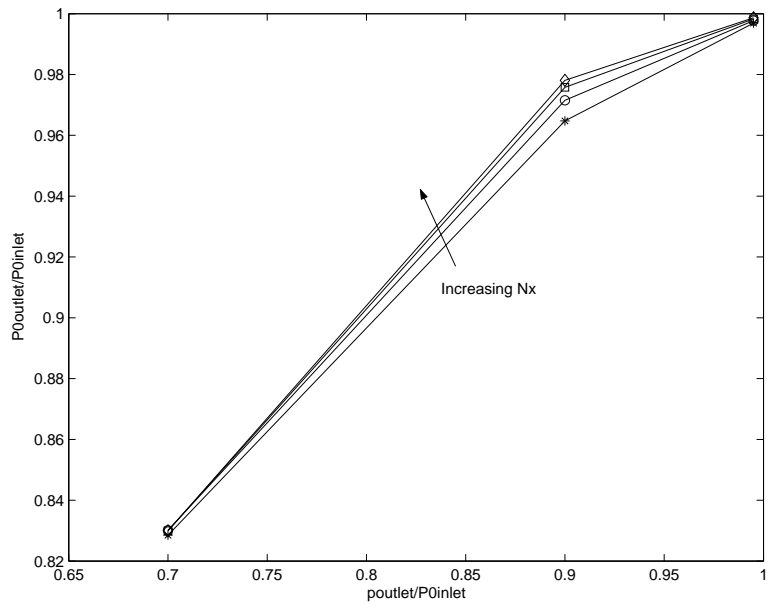


Figure 8: Outlet total pressure behavior with  $p_{outlet}/P_{0inlet}$  and  $N_x$ .

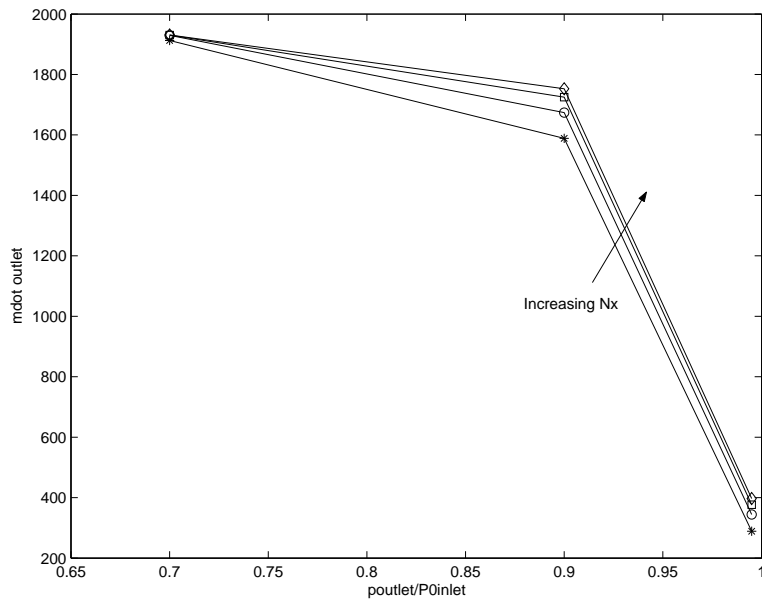


Figure 9: Outlet mass flow rate behavior with  $p_{outlet}/P_{0inlet}$  and  $N_x$ .